Synthesis of CoOOH Hierarchically Hollow Spheres by Nanorod Self-Assembly through Bubble Templating

Jinhu Yang and Takehiko Sasaki*

Department of Complexity Science and Engineering, School of Frontier Sciences, The University of Tokyo, 5-1-5, Kashiwanoha, Kashiwa, Chiba 277-8561, Japan

Received October 4, 2007. Revised Manuscript Received December 12, 2007

CoOOH hierarchically hollow spheres consisting of nanorods by self-assembly coupled with bubble templating through a facile one-step hydrothermal route have been demonstrated. An energy-minimizing-driven self-assembly of CoOOH nanorods on the base of O_2 bubbles induced by CTAC is responsible for the formation of hierarchically hollow structure. The effects of H_2O_2 concentrations and CTAC during the crystallization and self-assembly process of CoOOH nanorods have been studied. It is found that H_2O_2 concentration is a key factor that affects not only the crystallinity, shape, and size but also the further self-assembly process of CoOOH nanorods, determining the final formations of hollow spheres or solid aggregates of nanorod self-assemblies, while CTAC can probably induce the CoOOH nanorods to get more ordered self-assembly. This is the first synthesis of complex hollow structure of CoOOH crystals with hierarchy.

Introduction

The strategy to manipulate the nanoscale building blocks via self-assembly and higher-ordered organization approaches into hierarchically complex architectures is a great challenge toward both material synthesis and advanced nanodevices.[1–13] In this process, self-assembly driven by chemical or physical interactions enables primary building units to form versatile flexible shapes.[14] In recent years, much attention has been paid particularly to the fabrication of hierarchically hollow structures including hollow spheres as well as polyhedrons by primary building unit self-assembly because the materials with such hollow structures have broadly potential applications in catalysis and drug delivery and as artificial cell and light fillers, etc.[15–23] However, among all of the reports, the successes are mainly limited to metal and oxide systems; it is necessary to extend the scopes to other kinds of functional materials, from the viewpoint of application. On the other hand, the curved structures built from self-assembly of the primary building blocks, such as hollow spheres, are demanded in new technologies;[15,24,25] although many progresses have been made,[15–19,21,22] the facile and effective routes are still required for systematic studies of self-assembly behaviors. For this reason, herein we develop a facile, one-step hydrothermal route to the synthesis of CoOOH hierarchically hollow spheres by combining nanorod self-assembly and bubble templating.

Cobalt oxide and hydroxide have attracted great interests due to their unique physical and chemical properties with potentials in magnetics,[26–28] catalysis,[29–31] electrochemistry,[32–39]

* Corresponding author. E-mail takehiko@k.u-tokyo.ac.jp.

(1) Whitesides, G. M.; Grzybowski, B. *Science* **2002**, *295*, 2418.
(2) Fan, H.; Yang, K.; Boye, D. M.; Sigmon, T.; Malloy, K. J.; Xu, H.; Lopez, G. P.; Brinker, C. J. *Science* **2004**, *304*, 567.
(3) Garcia-Ruiz, J. M.; Hyde, S. T.; Carnerup, A. M.; Christy, A. G.; Van Kranendonk, M. J.; Welham, N. J. *Science* **2003**, *302*, 1194.
(4) Whang, D.; Jin, S.; Wu, Y.; Lieber, C. M. *Nano Lett.* **2003**, *3*, 1255.
(5) Yang, J. H.; Qi, L. M.; Lu, C. H.; Ma, J. M.; Hu, M. C. *Angew. Chem., Int. Ed.* **2005**, *44*, 598.
(6) Park, S.; Lim, J. H.; Chung, S. W.; Mirkin, C. A. *Science* **2004**, *303*, 348.
(7) Mann, S.; Cölfen, H. *Angew Chem., Int. Ed.* **2003**, *42*, 2350.
(8) Feng, X. J.; Zhai, J.; Jiang, L. *Angew. Chem., Int. Ed.* **2005**, *44*, 5115.
(9) Zhang, W. Q.; Xu, L. Q.; Tang, K. B.; Li, F. Q.; Qian, Y. T. *Eur. J. Inorg. Chem.* **2005**, 653.
(10) Fang, X. S.; Ye, C. H.; Zhang, L. D.; Zhang, J. X.; Zhao, J. W.; Yan, P. *Small* **2005**, *1*, 422.
(11) Liang, J. B.; Liu, J. W.; Xie, Q.; Bai, S.; Yu, W. C.; Qian, Y. T. *J. Phys. Chem. B* **2005**, *109*, 9463.
(12) Zhou, J.; Ding, Y.; Deng, S. Z.; Gong, L.; Xu, N. S.; Wang, Z. L. *Adv. Mater.* **2005**, *17*, 2107.
(13) Yuan, J. K.; Li, W. N.; Gomez, S.; Suib, S. L. *J. Am. Chem. Soc.* **2005**, *127*, 14184.
(14) Mo, M. S.; Yu, J. C.; Zhang, L. Z.; Li, S.-K. A. *Adv. Mater.* **2005**, *17*, 756.
(15) Caruso, F.; Caruso, R. A.; Möhwald, H. *Science* **1998**, *282*, 1111.
(16) Dinsmore, A. D.; Hsu, M. F.; Nikolaides, M. G.; Marquez, M.; Bausch, A. R.; Weitz, D. A. *Science* **2002**, *298*, 1006.
(17) Bigi, A.; Boanini, E.; Walsh, D.; Mann, S. *Angew. Chem., Int. Ed.* **2002**, *41*, 2163.
(18) Yuan, J.; Laubernds, K.; Zhang, Q.; Suib, S. L. *J. Am. Chem. Soc.* **2003**, *125*, 4966.
(19) Liu, B.; Zeng, H. C. *J. Am. Chem. Soc.* **2004**, *126*, 8124.
(20) Gao, P. X.; Wang, Z. L. *J. Am. Chem. Soc.* **2003**, *125*, 11299.
(21) Cong, H. P.; Yu, S. H. *Adv. Funct. Mater.* **2007**, *17*, 1814.
(22) Yu, D. B.; Sun, X. Q.; Zou, J. W.; Wang, Z. R.; Wang, F.; Tang, K. *J. Phys. Chem. B* **2006**, *110*, 21667.
(23) Gao, S. Y.; Zhang, H. J.; Wang, X. M.; Deng, R, P.; Sun, D. H.; Zheng, G. L. *J. Phys. Chem. B* **2006**, *110*, 15847.
(24) Sun, Y.; Xia, Y. *Science* **2002**, *298*, 2176.
(25) Goldberger, J.; He, R.; Zhang, Y.; Lee, S.; Yan, H.; Choi, H.-J.; Yang, P. *Nature (London)* **2003**, *422*, 599.
(26) Kurmoo, M. *Chem. Mater.* **1999**, *11*, 3370.
(27) Kurmoo, M.; Kumagai, H.; Hughes, S. M.; Kepert, C. *J. Inorg. Chem.* **2003**, *42*, 6709.
(28) Feyerherm, R.; Loose, A.; Rabu, P.; Drillon, M. *Solid State Sci.* **2003**, *5*, 321.
(29) (a) Auschitzky, E.; Boffa, A. B.; White, J. M.; Sahin, T. *J. Catal.* **1990**, *125*, 325. (b) Thormahlen, P.; Skoglundh, M.; Fridell, E.; Andersson, B. *J. Catal.* **1999**, *188*, 300.
(30) Radwan, N. R. E.; Mokhtar, M.; El-Shobaky, G. A. *Appl. Catal. A: Gen.* **2003**, *241*, 77.
(31) Dinamani, M.; Kamath, P. V. *J. Appl. Electrochem.* **2000**, *30*, 1157.

10.1021/cm702868u CCC: $40.75
Published on Web 01/16/2008

and sensing devices.[40–43] As an important electrode material, CoOOH had been often used as an effective additive in Ni/metal hydride (Ni/MH) batteries for achieving better performances,[35–39] which depends on technically coating CoOOH on the NiOOH surfaces to improve the capacity and conductivity of NiOOH because of higher conductivity of CoOOH. Therefore, the good dispersion of CoOOH particles on NiOOH surfaces is crucial because the better contacts of two different hydroxides relate closely to the better performance of the battery, which requires the shape and size control on CoOOH material before use. Aiming at this goal, some attempts including direct solution precipitation,[39,43,44] precursor conversions,[35b,36d] and electrochemical deposition[45] have been made for the preparation of CoOOH; however, at present, the controlled synthesis of CoOOH is still a big challenge for researchers. In addition, CoOOH is also an active material as gas sensor.[43] To get higher sensitivity, for a given sensing material, besides the large surface area, an open porous structure even at micrometer scale was evidenced to be beneficial in sensing molecules due to its easy accessibility, thereby enhancing the molecular contact and transport kinetics.[46] Our controlled synthesis of the CoOOH hierarchically hollow spheres consisting of nanorods provides the advantages of uniform shape and size (~100 nm in length and ~15 nm in thickness) and continuous open porous structures. These factors may be favorable for achieving better performances in Ni/MH batteries facilitated by sonication to get good nanorod dispersion and gas sensors.

Experimental Section

Preparation of CoOOH Hollow Spheres. A 9 mL solution containing *N*,*N*-dimethylformamide (DMF), acetonitrile (MeCN), and water with the volume ratio of 1:1:1 was prepared in a 25 mL Teflon autoclave, and then 0.003 g of $CoCl_2$ and 0.012 g of hexadecyltrimethylammonium chloride (CTAC) were added under stirring, resulting a homogeneous pink solution. After 2 mL of H_2O_2 (30%) was added with slight stirring, the reaction solution was kept in oven at 150 °C for 20 h, giving a brown precipitation. Reaction conditions were optimized as described in the Results and Discussion section. The concentrations of $CoCl_2$, CTAC, and H_2O_2 in solution are 2.5 mM, 8 mM, and 1.6 M, respectively. Then, the Teflon autoclave was cooled to room temperature, and the product was collected with the centrifuge method, redispersed by sonication, washed using water three times, and finally dried in air, preparing for characterizations.

Characterization. Scanning electron microscopy (SEM) measurements were performed with a JSM-5510LV microscope operated at 10 kV, and transmission electron microscopy (TEM) observations were conducted on a JEOL JEM-2010F microscope operated at 200 kV combined with an energy dispersive X-ray (EDX) analyzer at the Institute for Solid State Physics, the University of Tokyo. Powder X-ray diffraction (XRD) patterns were recorded on a Rigaku RINT-2500V diffractometer with Cu Kα radiation ($\lambda = 1.5406$ Å) at a scanning speed of 0.1°/s over 2θ range of 10–80°. Raman spectra were measured on a RENISHAW Raman spectroscope excited at 514 nm by an Ar^+ laser (25 mW); the irradiation power at the sample position was measured to be 0.18 mW. X-ray photoelectron spectra (XPS) were measured using Rigaku XPS-7000 with Mg Kα radiation (10 kV, 30 mA).

Results and Discussion

Characterization of CoOOH Hierarchically Hollow Spheres. The typical SEM image of the product shown in Figure 1a displays that spherical CoOOH crystals are formed in large scale with relatively good dispersion and uniform diameters of ~500 nm. Moreover, observing from some broken spheres, it is evident that these CoOOH spheres are in hollow structure with loose shells. The XRD pattern (Figure 1B) of the CoOOH hollow spheres shows several diffraction peaks corresponding to the rhombohedral heterogenite structure with cell parameters $a = 2.829$ and $c = 13.13$ Å (JCPDS Card No. 14-0673. JCPDS: Joint Committee on Powder Diffraction Standards), which confirms that these hollow spheres are pure CoOOH. Relatively broadened diffraction peaks indicate the CoOOH crystals constituting hollow spheres are in small sizes. Furthermore, the CoOOH hollow spheres were characterized with TEM to examine their fine structures. An overview TEM image in Figure 1C presents that the hollow spheres are well dispersed and possess the average diameters less than 500 nm, which is in good agreement with SEM observation. Closer inspection of the sample (Figure 1D) reveals that lots of CoOOH nanorods arrange in a manner constituting circular shells and, therefore, forming hollow spheres.

A series of characterizations other than XRD measurements were conducted for the phase analysis of typical CoOOH hollow spheres. The EDX analysis (Figure 2A) gives clear peaks corresponding to elements of Co and O besides Cu originated from TEM copper grid, indicating the hollow spheres are made of Co and O elements. The Raman spectrum in Figure 2B displays two strong peaks at 499 and 684 cm^{-1} and one weak peak at 635 cm^{-1}, which agree well with that of the CoOOH films prepared via chemical and electrochemical routes at relatively high temperature.[45]

(32) Poizot, P.; Laruelle, S.; Grugeon, S.; Dupont, L.; Tarascon, J. M. *Nature (London)* **2000**, *407*, 496.
(33) Sood, A. K. *J. Appl. Electrochem.* **1986**, *16*, 274.
(34) Li, W. Y.; Xu, L. N.; Chen, J. *Adv. Funct. Mater.* **2005**, *15*, 851.
(35) (a) Pralong, V.; Delahaye-Vidal, A.; Beaudoin, B.; Leriche, J.-B.; Tarascon, J.-M. *J. Electrochem. Soc.* **2000**, *147*, 2096. (b) Barde′, F.; Palacin, M.-R.; Beaudoin, B.; Delahaye-Vidal, A.; Tarascon, J.-M. *Chem. Mater.* **2004**, *16*, 299.
(36) (a) Lichtenberg, F.; Kleinsorgen, K. *J. Power Sources* **1996**, *62*, 207. (b) Lim, H. S.; Stadnick, S. J. *J. Power Sources* **1989**, *27*, 69. (c) Aravamuthan, S.; Annamma, C. V.; Pillai, N. R.; Nair, M. J. *J. Power Sources* **1994**, *50*, 81. (d) Hosono, E.; Fujihara, S.; Honma, I.; Ichihara, M.; Zhou, H. S. *J. Power Sources* **2006**, *158*, 779.
(37) (a) Zimmerman, A. H.; Seaver, R. *J. Electrochem. Soc.* **1990**, *137*, 2662. (b) Oshitani, M.; Yufu, H.; Takashima, K.; Tsuji, S.; Matsumaru, Y. *J. Electrochem. Soc.* **1989**, *136*, 1590.
(38) Li, X. F.; Xia, T. C.; Dong, H. C.; Wei, Y. W. *Mater. Chem. Phys.* **2006**, *100*, 486.
(39) Wu, W.; Gao, X.; Geng, M.; Gong, Z.; Noreus, D. *J. Phys. Chem. B* **2005**, *19*, 5392.
(40) Cao, A.-M.; Hu, J. S.; Liang, H. P.; Song, W. G.; Wan, L. J.; He, X. L.; Gao, X. G.; Xia, S. H. *J. Phys. Chem. B* **2006**, *110*, 15858.
(41) Nam, H.-J.; Sasaki, T.; Koshizaki, N. *J. Phys. Chem. B* **2006**, *110*, 23081.
(42) Cantalinia, C.; Postb, M.; Busoc, D.; Guglielmic, M.; Martuccic, A. *Sens. Actuators, B* **2005**, *108*, 184.
(43) Wu, R.-J.; Wu, J.-G.; Tsai, T.-K.; Yeh, C.-T. *Sens. Actuators, B* **2006**, *120*, 104.
(44) Delahaye-Vidal, A.; Beaudoin, B.; Ge′rand, B.; Tarascon, J. M. *J. Mater. Chem.* **1999**, *9*, 955.
(45) Pauporte, T.; Mendoza, L.; Cassir, M.; Bernard, M. C.; Chivote, J. *J. Electrochem. Soc.* **2005**, *152*, C49.
(46) Qiu, Y. F.; Yang, S. H. *Adv. Funct. Mater.* **2007**, *17*, 1345.

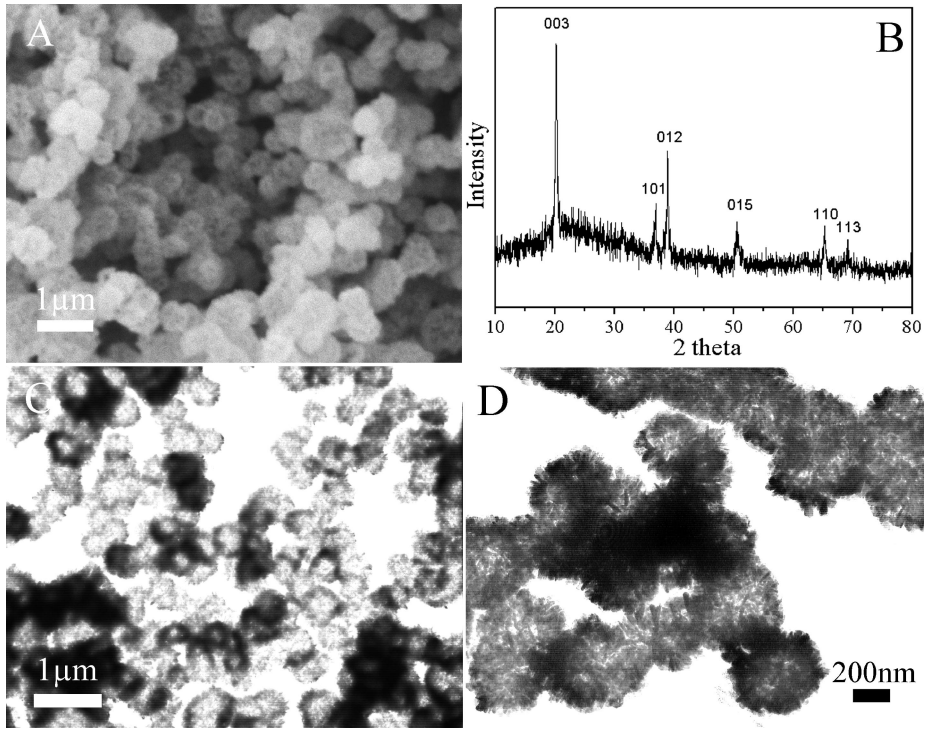

Figure 1. SEM image (A), XRD pattern (B), and TEM images (C, D) of CoOOH (cobalt oxyhydroxide) hollow spheres. Prepared in the condition of $[H_2O_2] = 1.6$ M.

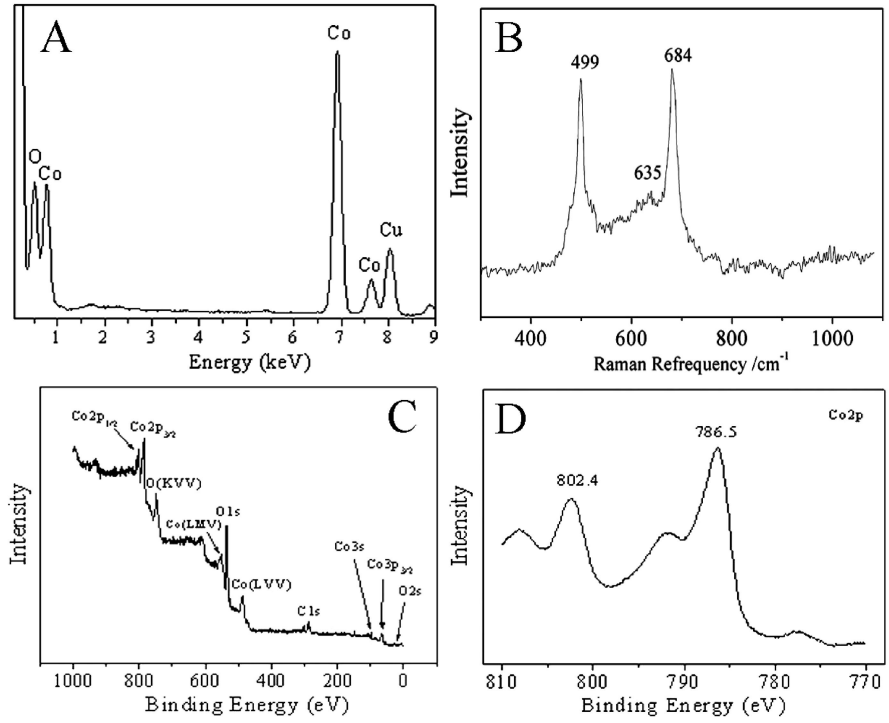

Figure 2. EDX analysis (A), Raman spectrum (B), and XPS analyses (C, D) of CoOOH hollow spheres.

Furthermore, the wide scan XPS spectrum (Figure 2C) for CoOOH hollow spheres shows typical peaks corresponding to the binding energy ranges of Co 2p, 3s, 3p and O 1s and 2s, respectively, as well as C 1s coming from surfactant CTAC, which suggests the existence of CTAC molecules in hollow spheres even after washing and sonication processes. Moreover, the selected XPS spectrum in the range of 770−810 eV displays peaks clearly at 786.5 and 802.4 eV, which are assigned as Co $2p_{3/2}$ and $2p_{1/2}$, respectively. In principle, for a given core electron, its binding energy increases with the increase of its atomic valence, which is applicable well to cobalt compounds. Table 1 lists binding energy of Co 2p for different Co compounds. It is obvious that for these different cobalt compounds, with the valence of Co increase from 0 to 3+, the corresponding binding energy of Co 2p increase gradually from 778.2 to 786.5 eV ($2p_{3/2}$) and 793.2 to 802.4 eV ($2p_{1/2}$), respectively.[47] According to this tendency, it is certain that the valence of Co

Table 1. Binding Energy (eV) for Co Metal, Oxide, and Hydroxides

spectral region	Co metal[a]	CoO[a]	$Co(OH)_2$[a]	as-synthesized CoOOH
Co $2p_{3/2}$	778.2	780.5	781.3	786.5
Co $2p_{1/2}$	793.2	796.3	797.3	802.4

[a] From ref 47.

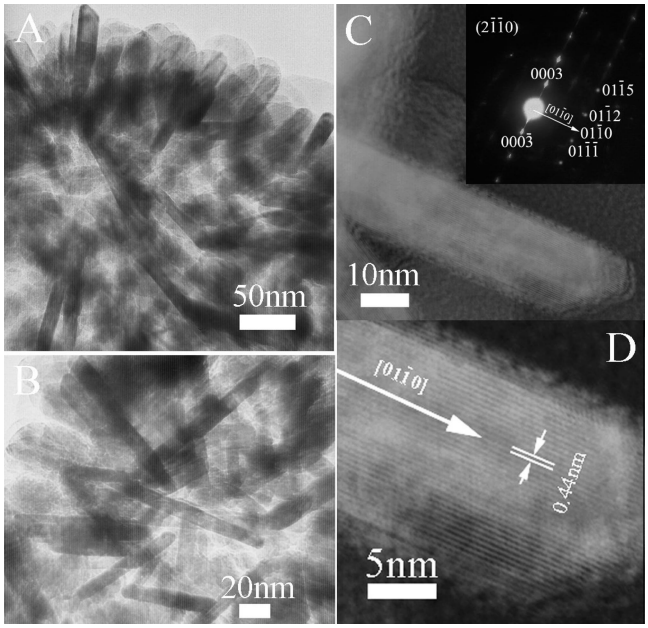

Figure 3. TEM images of CoOOH hollow sphere (A, B) after sonication and a single nanorod (C, D) from hollow sphere. Inset is ED pattern corresponding to the single nanorod in (C).

element in the sample is 3+. Therefore, the sample of hollow sphere is pure CoOOH, which confirms well the XRD results.

To image the interior architecture of the CoOOH hollow spheres and the crystal structures of nanorods, the sample was investigated by high-magnification TEM after being processed by sonication for 10 min. Figure 3A,B shows that the hollow spheres are partially broken after sonication. It can be seen clearly that the hollow sphere consists of orderly arranged nanorods in a parallel manner (upside in Figure 3A) and the nanorods hold uniform sizes with length ~100 nm and thickness ~15 nm (Figure 3B,C), resulting in an average aspect ratio of ~7. The corresponding electron diffraction (ED) pattern of single nanorod (inset in Figure 3C) exhibits a set of sharp spots corresponding to {0003} reflections equivalent to 0.44 nm of *d*-spacing, which is consistent with the XRD result where (0003) reflection is intensified, and several additional sets of weak spots with spacings of 0.242, 0.231, and 0.180 nm corresponding to $\{01\bar{1}\bar{1}\}$, $\{01\bar{1}2\}$, and $\{01\bar{1}5\}$ reflections, respectively. In addition, the high-resolution TEM observation in Figure 3D for the nanorod also displays clear crystal lattices with spacing of 0.44 nm, corresponding to {0003} planes, which agrees well with the indexes in ED pattern. This result indicates that the CoOOH nanorod is a single crystal and the growth direction is perpendicular to ⟨0003⟩, which is the same as that of CoOOH nanorods prepared through a different route,[39] suggesting the formation of such oriented nanorods might be due to the crystal habit of CoOOH itself.

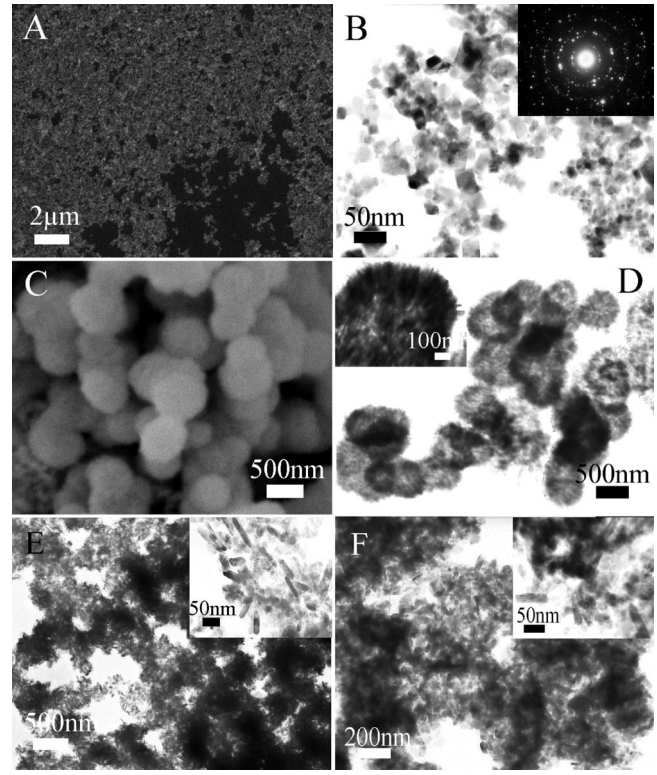

Figure 4. SEM images (A, C) and TEM images (B, D−F) of CoOOH nanocrystals synthesized at the different H_2O_2 concentrations. [H_2O_2]: (A, B) 0 M, (C, D) 0.88 M, (E) 2.2 M (F) 2.7 M. ED pattern (B) and partially enlarged TEM images (D−F) are inserted in the corresponding figures.

According to the geometrical relation, it is readily indexed that the CoOOH nanorod grows along the $[01\bar{1}0]$ direction with side faces equivalent to $\{2\bar{1}\bar{1}0\}$, as shown in Figure 3C. This is the first synthesis of CoOOH hollow spheres with hierarchy (single nanorod → nanorod assembly → hollow sphere) consisting of orderly self-assembled nanorods. In other metal[6] or oxide[19] systems similar hierarchical structures have been reported.

Effects of H_2O_2 Concentrations and CTAC. It is found that H_2O_2 concentration has a remarkable effect on the morphology, structure, and phase of CoOOH crystals, as shown in Figure 4. When no H_2O_2 was employed, a layer of dense-laid nanoparticles on the substrate with an average size below 20 nm was formed (Figure 4A,B), other than hierarchically hollow spheres under typical condition. The ED pattern in Figure 4B displays several sets of distinct diffraction rings with *d*-spacings corresponding well to the cubic structure of Co_3O_4, revealing that the nanoparticles are actually made of Co_3O_4, which is also confirmed by the corresponding XRD pattern (JCPDS Card No. 43-1003) (Figure 5A). The formation of Co_3O_4 may be ascribed to the oxidation by trace amount of dissolved O_2 from air in solution without H_2O_2, and at a relatively low H_2O_2 concentration (0.88 M), the pure CoOOH crystals were produced (Figure 5B) due to oxidation by excess H_2O_2 with respect to the stoichiometric ratio. The CoOOH spheres (Figure 4C) look homogeneous in contrast and solidlike, possessing a diameter of 500 nm that is typical for hollow spheres in Figure 1. However, the further TEM characterization indicates that these spheres are still in hollow structure

(47) Chuang, T. J.; Bidle, C. R.; Rice, D. W. *Surf. Sci.* **1976**, *59*, 413.

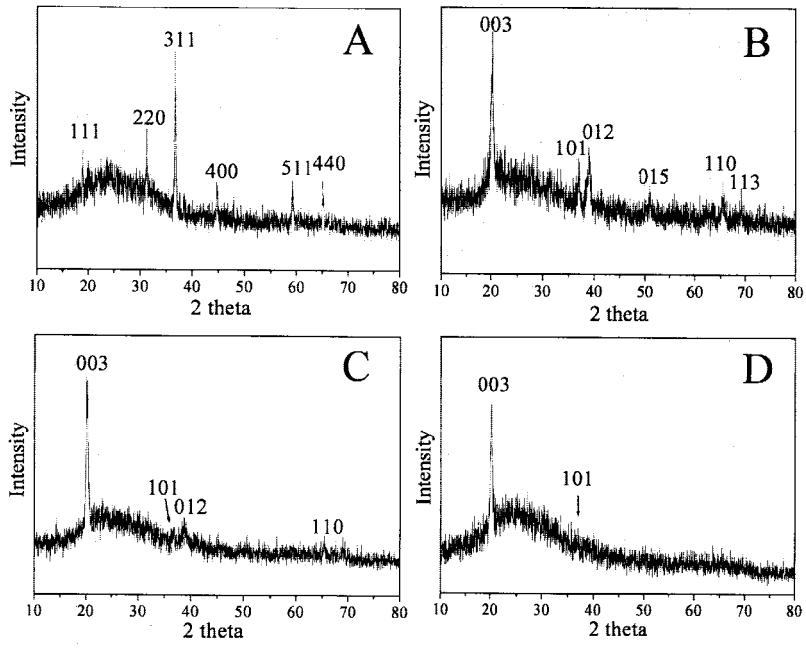

Figure 5. XRD patterns of CoOOH nanocrystals synthesized at the different H_2O_2 concentrations. [H_2O_2]: (A) 0, (B) 0.88, (C) 2.2, and (D) 2.7 M.

and self-assembled by nanorods with a little longer length ~150 nm, but just in a more dense and ordered way (Figure 4D). In addition, the analysis of nanorods represents the same growth direction of [$01\bar{1}0$] and side face ($2\bar{1}\bar{1}0$) as the typical ones. As demonstrated above, the obvious CoOOH hollow spheres with a little loose self-assembly were prepared by increasing the H_2O_2 concentration to 1.6 M (Figures 1 and 3), implying a tendency that self-assembling behavior of CoOOH nanorods would become weak with increasing H_2O_2 concentration. Further increase of the H_2O_2 concentration to 2.2 M resulted in the formation of nonuniform solid aggregates of CoOOH nanorods, accompanied by a great number of monodispersed individual nanorods with average length of 80 nm (Figure 4E). When the H_2O_2 concentration was finally increased to 2.7 M, the aggregates got much looser, leading to more nanorods dispersing aside from aggregates (Figure 4F). From the high-magnification image (inset of Figure 4F) the nanorods turned to be more irregular in shape and smaller in size.

In the past decades, many reports have been given to surfactant-templated routes to prepare hollow structured materials because surfactants could form diverse assemblies in solution and be used as templates. To examine whether CTAC had exerted an influence on the formation of the CoOOH hollow spheres, a synthesis in the absence of CTAC was conducted with other conditions being typical. SEM and TEM images in Figure 6 reveal that the CoOOH hollow spheres self-assembled by nanorods could be formed even without CTAC and that the sizes of CoOOH nanorods (Figure 6C, inset) are essentially the same as those in typical condition (Figure 3), suggesting that the presence of CTAC had neither templating function for hollow sphere formation nor obvious contribution to shape control of CoOOH nanorods. However, through fine comparison, it was found that the self-assembly of CoOOH nanorods got much disordered without CTAC, leading to CoOOH hollow spheres formed here looking more loose and irregular than that of typical spheres. This result implies that the existence of CTAC is beneficial for the CoOOH nanorods self-assembling in a more ordered and tight manner to form regular hollow spheres, where CTAC molecules probably form interparticle bilayers inducing the CoOOH nanorods gluing together parallelly during the self-assembly process. In fact, such similar self-assemblies assisted by organic molecules such as micromolecules and surfactants as organic connectors to link inorganic building blocks to produce nanoparticle-based superstructures have been reported.[7] Hence, with respect to the formation of CoOOH hollow spheres self-assembled by nanorods in this work, we believe that the crystallinity, uniform shape, and size of CoOOH nanorods afford structure match and spatial proximity to realize effective self-assembly induced by CTAC molecules. This self-assembly process is likely driven by energy minimization for the surfaces of nanorods. It should explain that the structure match proposed here refers to the match of crystal lattice at atomic scale, for example, the better structure match from the identical side faces, {$2\bar{1}\bar{1}0$} of CoOOH nanorods, which relates closely to the crystallinity of CoOOH nanorods.

Reaction Mechanism. Under the conditions of our experiments, the following reactions are thought to occur in solution.

$$2H_2O_2 \rightarrow 2H_2O + O_2\uparrow \quad (1)$$

$$2CoCl_2 + 3H_2O_2 \rightarrow 2CoOOH + 4HCl + O_2\uparrow \quad (2)$$

According to the reactions 1 and 2, O_2 could be generated from reactions of both $CoCl_2$ oxidation by H_2O_2 and decomposition of H_2O_2 itself. And this might enable the possibility of reaction 3 in theory that starting material of $CoCl_2$ oxidized directly by O_2 to CoOOH, since there are a large amount of O_2 molecules existing in solution.

$$4CoCl_2 + O_2 + 6H_2O \rightarrow 2CoOOH + 8HCl \quad (3)$$

However, because the amount of H_2O_2 used is superfluous relative to $CoCl_2$ (1.6 M/2.5 mM), we deem that the reaction

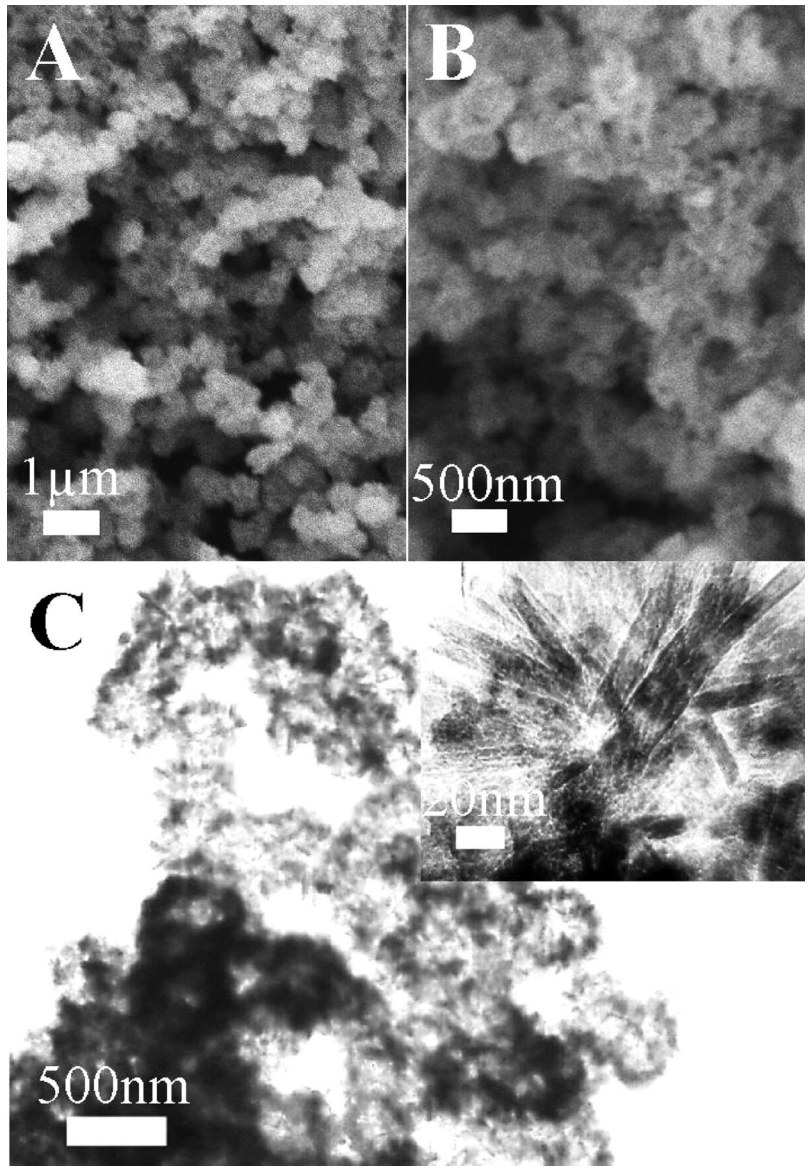

Figure 6. SEM (A, B) and TEM (C) images of CoOOH hollow spheres formed in the absence of CTAC. Inset in (C) is magnified TEM image of CoOOH nanorods. Prepared in the condition of $[H_2O_2] = 1.6$ M.

2 is dominating in oxidation relative to reaction 3 and responsible for the formation of CoOOH crystals and hollow structure in conjunction with reaction 1. Notably, from the experimental results above, we found that CoOOH hierarchically hollow spheres self-assembled by nanorods are preferentially formed at relatively low H_2O_2 concentrations (0.88−1.6 M), whereas nanorod solid aggregates are preferred at relatively high H_2O_2 concentrations (2.2−2.7 M). It should be pointed out that high concentrations of H_2O_2 can not only give rise to the concentration of O_2 that subsequently form more gas bubbles but also increase the reaction rates, for example, the nucleation and growth rates of CoOOH, which could greatly affect the crystallinity and morphology and further self-assembly of crystals.

In general, pressure is an important parameter especially for the hydrothermal synthetic route because hydrothermal reaction provides not only high temperature but also high pressure sometimes. To better understand the real situations of reaction process, we calculated that the systematic pressure is about 35 atm in the typical synthesis based on some presumptions (see Supporting Information). And the pressure was proven to be a significant factor for the final phase of product in our synthetic system: if a large-sized Teflon autoclave (100 mL) was employed instead of the present one (25 mL) with other conditions being the same, accompanying inevitably the decrease of total pressure inside the Telfon autoclave (15.49 atm), the pure Co_3O_4 nanocubes with average diameters about 120 nm were produced instead of CoOOH crystals (Figure S1). According to our calculations, more than 95% of each solvent (water, DMF, and MeCN) remained in liquid solution, ensuring the full interactions of the solvents and CoOOH crystals to realize the effective structure and phase control of CoOOH crystals; and second, the total pressure could be adjustable, not limited by changing a volume of an autoclave only, by simply varying the H_2O_2 concentration, which may enlighten us to design the experimental details qualitatively. Of course, in the real situations, H_2O_2 cannot decompose completely, and perhaps, the azeotropes composed of the solvents would be formed, which

Scheme 1. Possible Mechanism for the Formation of CoOOH Hierarchically Hollow Spheres

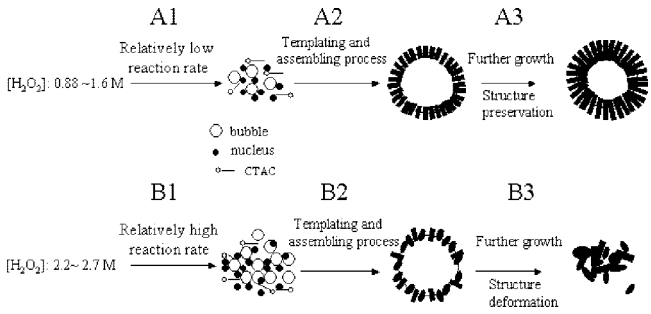

might lead to a little difference between the calculated and the real pressure.

Formation of Hollow Spheres vs Solid Aggregates. Based on the present results, a plausible proposition involving bubble-templating coupled with nanorod self-assembly process can be given briefly, where H_2O_2 worked as not only the oxidant but also the source to afford the templates of O_2 bubbles. Actually, the gas bubble templating method has been evidenced to be feasible and facile to fabricate hollow spheres of inorganic materials, such as ZnSe,[48a] ZnO,[48b] and $CaCO_3$.[48c] As illustrated in Scheme 1, when 0.88−1.6 M of H_2O_2 was present, the relatively low concentrations would lead to relatively low reaction rates. Driven by reactions 1 and 2, a certain concentration of O_2 was generated, forming sub-microbubbles in the current situation; simultaneously, a large amount of CoOOH nuclei was produced in solution through relatively low nucleation process according to reaction 2, leading to a relatively high local concentration of CoOOH nuclei (A1). Thus, it inevitably resulted in the CoOOH nuclei diffusing to the gas–liquid interfaces between O_2 bubbles and liquid solution. On the other hand, CTAC molecules tended to be enriched on the gas–liquid interfaces prompted by repulsion between their nonpolar ends and polar solvents because of their amphiphilic property. These two factors provide good possibility for the self-assembly of CoOOH nanorods under induction of CTAC molecules on the surfaces of O_2 bubbles. Subsequently, under continuous source feeding from solution during growth process the CoOOH nuclei grew into uniform nanorods with good crystallinity with side face of $(2\bar{1}\bar{1}0)$, which gives much better structure recognition for self-assembly. Therefore, driven by energy minimization, those CoOOH nanorods with uniform size and structure match self-assembled tightly in a parallel way to maximize the contact assisted by the surfactant CTAC on the gas–liquid interfaces between O_2 bubbles and liquid solution, leading to the formation of hollow structure (A2). Finally, the further growth gives the longer nanorods, which constitute the hierarchically hollow spheres by the self-assembly. Owing to the tight interactions between nanorods, the shape of hierarchically hollow sphere can be well preserved even after a series of treatment processes of the sample (A3). In contrast, at relatively high H_2O_2 concentration, the rates of O_2 generation and CoOOH nucleation and growth would be largely increased on the base of reactions 1 and 2, which thereby caused the formation of a great amount of bubbles as well as CoOOH nuclei in a short time (B1). However, in general, because the crystallizing partners need time to recognize each other and follow the lowest-energy path, fast crystallization often lead to kinetically controlled products such as metastable crystal structures or those with even defects,[48] probably resulting in a poor crystallinity of crystals. This principle was well evidenced here: judging from the XRD patterns of CoOOH crystals at different H_2O_2 concentrations (Figures 1B and 5B−D), it is obvious that the increase in H_2O_2 concentration (from 0.88 to 2.7 M) leads to the decrease in crystallinity of CoOOH nanorods; in addition, CoOOH rods at high H_2O_2 concentration (2.2−2.7 M) appeared a little irregular in shape and vague in outline, confirming the poor crystallinity as well. Apparently, these are unfavorable for self-assembly process because they gave poor structure match and bad spatial proximity. As a result, although the similar self-assembly behavior occurred at relatively high H_2O_2 concentration, however, the intermediate products (B2) were only unstable self-assemblies of hollow spheres through weak contact of irregular nanorods due to the reason given above. During the further growth of CoOOH nanorods into larger size ones, the weak interactions between nanorods got much worse as a consequence of increased mismatch and unfavored recognition due to the irregular larger-size nanorods; the hollow structure would eventually deform into solid aggregates (B3).

In addition, the sizes of CoOOH hollow spheres and solid aggregates are similar, i.e., roughly 500 nm (hollow spheres) and a little smaller (aggregates), respectively, confirming the proposition involving an O_2 bubble-templating process. Besides, we noted that not only nanorod crystallinity but also the average size would decrease with increasing H_2O_2 concentration (0.88−2.7 M) (Figures 3 and 4D−F), for example, decrease from 150 to 100 nm and finally to less than 80 nm. Actually, it is easily understandable because, first, higher H_2O_2 concentration gives higher nucleation rate of CoOOH and generates more crystalline nuclei and nucleation sites at the initial stage of reaction and, second, the reactant of $CoCl_2$ to supply Co^{2+} ions to form CoOOH was fixed and insufficient compared with H_2O_2, which should lead to the smaller size of each nanorod in average. Taking together, the proposed mechanism can explain well the formation of CoOOH hierarchically hollow spheres.

Effects of Temperature, Reaction Time, and Solvents (DMF and MeCN). It was found that the relatively higher temperature and longer reaction time are favorable for the formation of well-crystallized CoOOH nanorods. Briefly, if the temperature is a little lower, such as 110 °C, the product were in bad crystallinity and bad assembly state. However, the temperature over 150 °C would exceed upper temperature limitation for a Teflon autoclave used; therefore, 150 °C was adopted in our synthesis. On the other hand, enough reaction time was crucial for the crystallinity of CoOOH nanorods, which is important for the ordered self-assembly of nanorods

(48) (a) Peng, Q.; Dong, Y. J.; Li, Y. D. *Angew. Chem., Int. Ed.* **2003**, *42*, 3027. (b) Yan, C. L.; Xue, D. F. *J. Alloys Compd.* **2007**, *431*, 241. (c) Hadiko, G.; Han, Y. S.; Fuji, M.; Takahashi, M. *Mater. Lett.* **2005**, *59*, 2519.

(49) (a) Yang, J. H.; Liu, G. M.; Lu, J.; Qiu, Y. F.; Yang, S. H. *Appl. Phys. Lett.* **2007**, *90*, 103109. (b) Li, F.; Ding, Y.; Gao, P. X.; Xin, X. Q.; Wang, Z. L. *Angew. Chem., Int. Ed.* **2004**, *43*, 5238.

to hollow spheres, as discussed above. To get better crystallinity of CoOOH nanorods, the reaction time was required at least up to 12 h, and there was no obvious effect on crystallinity and self-assemblies of nanorods if the time was longer than 20 h. In addition, we found the existence of both DMF and acetonitrile in the reaction system is indispensable to the formation of CoOOH hollow structure and even CoOOH phase. As shown in Figures S2 and S3, being other conditions typical, CoOOH solid spheres mixed with minor parts of Co_3O_4 cubes were formed if without DMF, and $Co(OH)_3$ nanobelts with unreported structural model yet were produced just in the absence of acetonitrile, which demonstrats that this synthetic system is rather versatile and could be adopted with promise to synthesize other inorganic crystals besides cobalt hydroxides.

Conclusions

We have successfully synthesized the CoOOH hierarchically hollow spheres made of self-assembled nanorods through a facile one-step hydrothermal route. An energy-minimizing-driven self-assembly process of nanorods under the induction of CTAC molecules on the base of O_2 bubble templates leads to the formation of these CoOOH hierarchically hollow spheres. H_2O_2 concentrations play an important role in controlling the morphology and structure of CoOOH nanorods and thereby determining the subsequent self-assembly processes and the eventual structures of CoOOH self-assemblies. To the best of our knowledge, this is the first synthesis of such kind of hollow superstructure of CoOOH, which is possible to have potentials on some aspects such as Ni/MH batteries and gas sensor due to the uniform shape and size and ordered self-assembly of CoOOH nanorods.

Acknowledgment. J.Y. gratefully acknowledges the financial support from the Japan Society for the Promotion of Science (ID: 18•06080). T.S. acknowledges the support by a Grand-in-Aid for Scientific Research (No. 19550008) from JSPS. TEM and Raman scatting measurements were performed at the Institute for Solid State Physics, the University of Tokyo. XPS measurements were performed at the High Power X-ray Laboratory, Institute of Engineering Innovation, School of Engineering, the University of Tokyo.

Supporting Information Available: Figures S1−S3 and the calculations for the systematic pressures. This material is available free of charge via the Internet at http://pubs.acs.org.

CM702868U